Journal homepage: https://itce.vn.ua/en

Information Technologies and Computer Engineering **Vol. 23, No. 1. 2026**

Article's History: Received: 06.11.2025 Revised: 12.02.2026
Accepted: 26.03.2026 Published: 20.04.2026

ISSN 1999-9941; e-ISSN 2078-6387
UDC 004.4:004.5:622.3
DOI: 10.31649/vitce/1.2026.170

Application of deep learning methods to image processing and enhancement: A case study on seismic data

Ruslan Malikov*
Postgraduate
Institute of Geology and Geophysics of Azerbaijan National Academy of Sciences
AZ1143, 119 H. Cavid Ave., Baku, Azerbaijan
https://orcid.org/0009-0005-2126-1642

Abstract. The aim of this study was to evaluate the effectiveness of a modified encoder-decoder neural network architecture for denoising and image enhancement using synthetic and real data. The research methodology was based on a computational experiment and included training the model on synthetic images, quantitatively comparing the obtained results with the f-x deconvolution method and an alternative convolutional denoising model, and testing the robustness on real data with the presence of various noise characteristics. It was found that the applied denoising technique was characterised not only by reducing the noise component but also by preserving spatially significant image characteristics, including sharpness of edges, local transitions, morphology, and the relative positions of structural elements without signs of excessive smearing. A final comparison of the methods on synthetic test images showed that the average signal-to-noise ratio, peak signal-to-noise ratio, and multiscale structural similarity index for the proposed approach were 45.9 dB, 29.7 dB, and 0.99, respectively. For the f-x deconvolution method, the corresponding values were 31.5 dB, 23.9 dB, and 0.94, while for the alternative convolutional noise reduction model, the values were 20.9 dB, 18.4 dB, and 0.86. When applied to real data, the same enhancement behaviour was preserved, including the removal of pronounced noise contamination and derivation of a relatively clean signal without signal distortion. Depending on the input features, the method was accompanied by a decrease in intense noise masking, a reduction in residual noise, while maintaining a distinguishable signal structure, and reconstruction under conditions of a more complex spatial organisation of interference. Spectral analysis revealed a reduction in noise energy without disrupting the spectral configuration in the informative frequency range. The practical significance lies in the potential application of the proposed approach as a computational method for processing noisy images in systems designed for noise reduction and restoration of various data structures

Keywords: image restoration; image denoising; structural preservation; seismic image reconstruction; supervised learning

Introduction

In image restoration research, improving the quality of visual data was considered not only as a noise reduction task, but also as a broader problem of reconstructing image structure under various types of degradation. This approach stemmed from the fact that in real-world visual information processing scenarios, distortions were rarely limited to an isolated noise pattern, but were accompanied by loss of contours, weakening of textures, blurring of local intensity transitions, and deformation of subtle details. For this reason, image restoration had emerged as an independent field of computer vision, where the quality of the result was determined not only by the degree of noise suppression, but also by the ability of the model to preserve the spatial organisation of the image. B. Goyal *et al.* (2020) demonstrated that the transition from classical noise reduction methods to trainable models altered the approach to reproducing structural image elements. The authors emphasised that modern methods of visual data restoration were based not on local smoothing, but on modelling the spatial relationships between the degraded and target images. Further development of this area was driven by deep learning, specifically, convolutional neural networks. C. Tian *et al.* (2020) showed that such models formed a new stage in the development of noise reduction methods, providing a transition from manual feature construction to automatic learning of multi-level image representations. Within the framework of this approach, noise reduction was considered to be not only as a reduction of the noise component, but also as a restoration of visual structure, in which the result depended on the ability of the model to combine local analysis of pixel connections with a broader context to preserve edges, textures, and low-contrast

Suggested Citation:
Malikov, R. (2026). Application of deep learning methods to image processing and enhancement: A case study on seismic data. *Information Technologies and Computer Engineering*, 23(1), 170-182. doi: 10.31649/vitce/1.2026.170

*Corresponding author

details. A similar direction of generalisation was presented in the work of J. Mao *et al.* (2025), where digital noise reduction methods were considered as a consistent transition from filtering schemes to architectures oriented towards image reconstruction under conditions of complex degradation. Scientists showed that modern models were most effective in cases, where noise reduction was combined with the preservation of structural similarity between the reconstructed and original images.

In image restoration architectures, encoder-decoder models have become widespread. These models combined multi-level feature extraction with spatial restoration and were used in problems where, along with noise suppression, the reconstruction of hidden or weakened structural elements was required. In the study by Y. Cui *et al.* (2024), it was shown that updated convolutional networks for image restoration worked with spatially detailed representations and reproduced informative elements without pronounced smoothing. Researchers noted that the preservation of structure in such models was considered an independent condition for the quality of reconstruction. A similar aspect was considered in the work by N. Nazir *et al*. (2024), where it was shown that deep learning systems were evaluated not only by the degree of signal purification, but also by the ability to preserve diagnostically significant edges, density transitions, and local morphological details. This indicated that for various types of images, the methodological task lain in combining noise suppression with the preservation and restoration of image structure. Further development in this direction was associated with residual learning, diffusion and generative models. In the work of B. Xia *et al.* (2023), the diffusion model was considered as a tool for image restoration with various types of distortions. The authors showed that such an architecture ensured a consistent refinement of the visual structure during the reconstruction process. In the study of Z. Luo *et al.* (2025), diffusion reconstruction was presented as an independent modern direction of image restoration, in which the reconstruction process was associated with a step-by-step cleaning and stabilisation of the structural features of the image. In the work of Y.N. Imamverdiyev & F.I. Musayeva (2022), the potential of adversarial approaches for the formation of realistic visual representations was analysed. Scientists noted that such models were focused not only on eliminating defects, but also on reproducing a visually consistent image structure. The expansion of this research framework can be seen in the applied areas of processing specialised visual data.

In the work of S. Azizova *et al.* (2026), it was shown that one of the quality criteria for image restoration remained the correct reproduction of its structural and colour consistency. In this logic, seismic image processing was a special case of applying restoration models to data with a complex internal structure, where not only noise reduction was essential, but also the preservation of the continuity of reflections, weak signals, and the geometric consistency of useful structures. A study by M. Ding *et al.* (2024) demonstrated that the Swin Transformer, Convolutional Neural Network, U-Net (Swin-Conv-UNet) architecture was applicable to seismic denoising by combining deep feature extraction with the reconstruction of spatial details. The analysis established that seismic data can be considered an example for testing general approaches to modern image restoration on structurally complex material. A summary of the cited studies reveals that modern approaches to image restoration were increasingly focused not only on noise reduction, but also on restoring the structural integrity of the image. However, the extent to which the U-Net architecture was capable of combining noise reduction with the reconstruction of structurally significant elements in the presence of complex background noise and weakened useful signals remained insufficiently explored. The aim of the study was to evaluate the application of a modified U-Net encoder-decoder neural network architecture for image denoising and quality enhancement on synthetic and real data. To achieve this goal, the following objectives were formulated: analyse modern deep learning approaches to processing and restoring noisy images and determine the place of the U-Net architecture among reconstruction methods; perform a quantitative assessment of reconstruction quality on synthetic data; evaluate the model's performance on real data with various noise characteristics, using seismic images as an example; and perform a spectral analysis of the denoising results to determine the degree of image structure preservation.

Materials and Methods

The study was conducted from February 2025 to March 2026 as a computational experiment. The U-Net architecture proposed by O. Ronneberger *et al.* (2015) served as the methodological basis, applied as a baseline encoder-decoder model for restoring noisy images, while preserving local structures. Seismic data were considered as an applied example of noisy images to test the model's performance under conditions of complex signal structures and varying degrees of noise distortion. The methodological framework included forming a training set, constructing and training a neural network model on synthetic data, quantitatively evaluating the results, and then applying the trained network to real images with various noise characteristics. This allowed evaluation of the model both under controlled conditions and when transferred to real data. The study material consisted of synthetic and real images. The synthetic set was generated based on three-dimensional data constructed from one-dimensional reflectivity traces. These one-dimensional signals were transformed into volumetric structures by introducing geometric deformations, such as inclined areas, folded shapes, and faults. Once the clean volumes had been formed, noise of varying intensities and textures was added to the clean volumes, creating "noisy image/clean image" pairs used for network training. This approach prevented the network from adapting to a single fixed level of degradation and facilitated the creation of a generalised model stable to a wide range of noise scenarios. All images were normalised to a range from -1 to 1, ensuring comparability of amplitude characteristics and computational stability. To expand the variability of the training data, amplitude scaling coefficients were

additionally applied to change the overall intensity level of the synthetic images; the values were sampled within the range from 0 to 1. This allowed for the modelling of varying signal intensities and reduced the risk of overfitting at a fixed level of noise degradation.

The network architecture had a symmetrical "encoder-decoder" structure. The encoding section used successive convolutional blocks, including convolution, batch normalisation, and a nonlinear activation function, which ensured feature extraction with a gradual decrease in spatial resolution. In the decoding section, its sequential reconstruction was performed using transposed convolutions. The transfer of local spatial information between symmetric layers of the network was carried out via skip connections, which helped to preserve fine image details. In the output section, a residual block was additionally used, based on the concept of deep residual learning by K. He *et al.* (2016), to refine the reconstruction result. The output layer was a 1×1 convolution with linear activation to form the reconstructed image. The estimated noise was defined as the difference between the input noisy image and the reconstructed result; this was the form in which it was further used in the visual analysis of the results. The model was trained using a supervised learning scheme: a noisy image was fed as input, and its clean version was used as the target output. Parameter optimisation was performed using the Adam algorithm, which provided adaptive updating of network weights based on gradient information (Kingma & Ba, 2015). The mean absolute error (MAE) was used as the primary loss function, based on the results of H. Zhao *et al.* (2017), who demonstrated its suitability for preserving image boundaries and local features. Thus, the computational scheme was aimed not only at reducing the MAE, but also at preserving the structural integrity of the data.

To evaluate the quality of the model on synthetic data, a test set of 1,600 samples formed on the basis of 100 synthetic cubes was used. Since reference clean images were available for this data, the reconstruction efficiency was determined using the metrics of signal-to-noise ratio, peak signal-to-noise ratio, and multiscale structural similarity index. The use of the latter metric was based on the approach of Z. Wang *et al.* (2003), according to which structural similarity was an informative characteristic of image quality, when comparing reconstructed and reference data. The signal-to-noise ratio (SNR) metric was used to characterise the degree of noise suppression, the peak signal-to-noise ratio (PSNR) was used to assess the relationship between signal power and reconstruction error, and the multiscale structural similarity index measure (MS-SSIM) was used to analyse the preservation of the spatial organisation of the reconstructed image. Together, these metrics provided a quantitative assessment of noise suppression, reconstruction accuracy, and structure preservation. For comparative analysis, the proposed model was compared with two alternative approaches: the FXDECONV frequency-domain deconvolution method described in the works of L.L. Canales (1984) and N. Gülünay (1986), and the DnCNN architecture developed by K. Zhang *et al.* (2017). This comparison was consistent with further quantitative and visual analysis of the results on synthetic test images.

To test the model on real data, three seismic datasets were used: Kerry, Volve, and F3. The choice was determined by differences in noise intensity, its complexity, and readability of the useful signal, which allowed these datasets to be considered as three model testing scenarios: processing data with pronounced noise masking, reconstruction with a relatively low level of noise contamination, and processing images with a mixed nature of random and more coherent interference. When characterising the F3 dataset, the data presented by R.M. Silva *et al.* (2019) were taken into account, for Volve – the data on the deposit presented by T.J. Szydlik *et al.* (2006), and for Kerry – the results of the structural interpretation considered by W.D.M. Alotaby (2015). The choice of these sets was determined by the differences in the structural organisation of the main signal and noise characteristics, which made it possible to evaluate the stability of the model in conditions of heterogeneity of the input data. The estimated noise was calculated as the difference between the input noisy image and the reconstructed result. Since reference noise-free data were not available for real images, the quality of the reconstruction was estimated indirectly – by the nature of the suppression of the noise component, the visual evaluation of spatially significant structures and changes in the averaged Fourier amplitude spectra before and after processing. This analysis scheme corresponded to the subsequent interpretation of the results for Kerry, Volve and F3 as three modes of noise degradation of real data. The computational implementation of the model was carried out in the Python environment using the PyTorch library (PyTorch Foundation, USA). Computational experiments were conducted on an NVIDIA Quadro P5000 GPU (NVIDIA Corporation, USA). A complete training cycle took approximately 8 hours, with the average duration of one epoch being about 140 seconds. Applying the trained model to the full test dataset took approximately 1 hour. The methodology used was aimed at testing reconstruction accuracy, model robustness to varying noise intensities and structures, and the preservation of spatial and spectral image characteristics after denoising.

Results

Quantitative evaluation of synthetic image reconstruction quality

After training the model using the Adam algorithm, a quantitative evaluation of reconstruction quality was performed on blind synthetic test images (Kingma & Ba, 2015). A comparison of the proposed method with the classical FXDECONV method and the DnCNN convolutional architecture revealed differences in SNR, PSNR, and MS-SSIM metrics (Canales, 1984; Gülünay, 1986; Zhang *et al.*, 2017). These differences affected both the degree of noise suppression and the preservation of image morphology, including image sharpness, local texture modification, and the relative positions of structural elements. The corresponding average SNR, PSNR, and MS-SSIM values were presented in Table 1.

Table 1. Average SNR, PSNR, and MS-SSIM values for synthetic test images using different reconstruction methods

Metrics	Noisy	FXDECONV	DnCNN	The proposed method
SNR, dB	31.0	31.5	20.9	45.9
PSNR, dB	23.8	23.9	18.4	29.7
MS-SSIM	0.94	0.94	0.86	0.99

Source: developed by the author

As shown in Table 1, the highest average values for all three metrics were recorded for the proposed method. The most pronounced differences between the compared approaches were observed for SNR and MS-SSIM. For the proposed method, the SNR was 45.9 dB, while for the noisy input, FXDECONV, and DnCNN, it was 31.0, 31.5, and 20.9 dB, respectively. These results indicated that after reconstruction, the contribution of the useful signal to the final image increased not only compared to the original noisy data but also compared to the results of alternative methods. Comparison with the FXDECONV revealed a significant difference both in the absolute SNR value and in the nature of the reconstruction. With the proposed method, reconstruction was accompanied by a change in SNR toward better separation of noise from signal, while for FXDECONV, the final value remained close to the level of the original image. When compared with DnCNN, the SNR was lower not only compared to the result of the proposed method but also for the noisy input image. This indicated a different trade-off between noise suppression and preservation of the image's content. The same direction of differences persisted for MS-SSIM. For the proposed method, the value of this metric reached 0.99, while for the noisy input and FXDECONV it was 0.94, and for DnCNN – 0.86. This comparison showed that reconstruction in the proposed approach was accompanied by the preservation of the spatial organisation of the image at a level close to the reference one, which was consistent with the interpretation of MS-SSIM as an indicator of structural similarity at several scale levels (Wang *et al.*, 2003). In the compared methods, the structural correspondence either remained unchanged or decreased. The reduction in the residual noise level occurred simultaneously with the preservation of the relative sharpness of boundaries, local intensity transitions, and the overall morphology of the image. Thus, the differences between the methods were recorded not at a single particular level, but in two interrelated dimensions of reconstruction – the degree of noise reduction and the degree of structure preservation. Taken together, these results demonstrated that the proposed approach resulted in image reconstruction with a different level of residual noise compared to FXDECONV and DnCNN. Quantitative comparison was supplemented by a visual comparison of the reconstructed images. Figure 1 showed reference samples, noisy input data, and reconstruction results obtained using FXDECONV, DnCNN, and the proposed method. Preservation of boundaries and fine details in the reconstructed images was consistent with the use of residual refinement at the model output (He *et al.*, 2016).

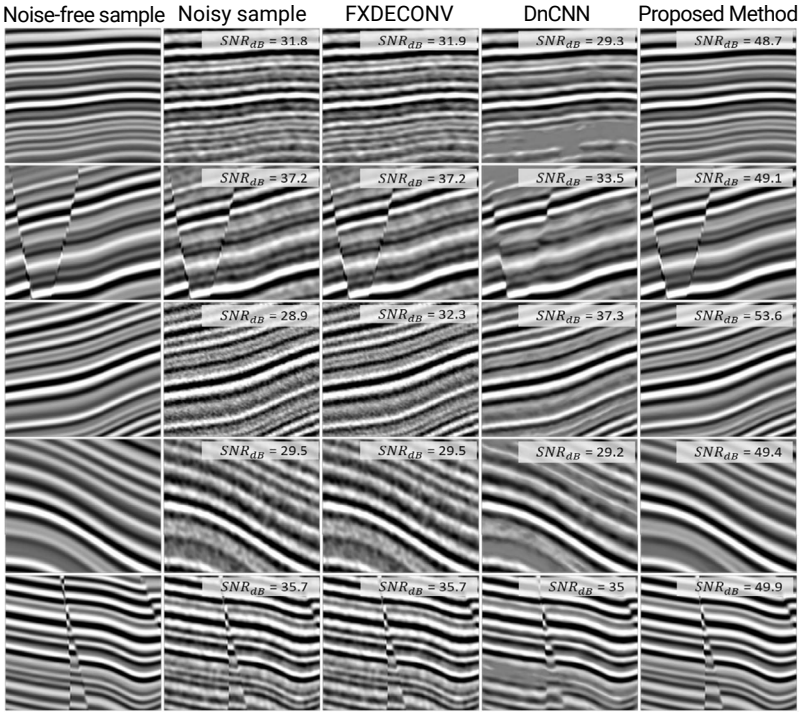

Figure 1. Visual comparison of synthetic test image reconstruction: reference image, noisy input, FXDECONV, DnCNN, and the proposed method

Source: based on L.L. Canales (1984), N. Gülünay (1986), K. Zhang *et al.* (2017)

As shown in Figure 1, the differences between the compared reconstruction options were evident not only in quantitative metrics but also in the visual reconstruction of the synthetic image structure. With the noisy input, SNR values ranged from 28.9 to 37.2 dB, while after applying the proposed method, the values increased to 48.7 to 53.6 dB. Moreover, the noise component in the original noisy images reduced the clarity of boundaries, blurred local transitions, and disrupted the continuity of reflective events. The FXDECONV method only partially reduced noise: in some samples, residual distortion, background inhomogeneity, and incomplete reconstruction of reflective boundary geometry remained, consistent with limited changes in SNR, PSNR, and MS-SSIM compared to the noisy input. The DnCNN results exhibited a different pattern of deviation, such as a reduction in the noise component with more pronounced smearing of local features, attenuation of fine details, and changes in the textural organisation of the image. Against this background, the reconstruction obtained by the proposed method was closest to the reference image, resulting in effective noise reduction with accurate preservation of edges, local contrasts, the continuity of reflective events, and the configuration of fine details without introducing excessive smoothing. Thus, the results on synthetic test images demonstrated a consistent advantage of the proposed method over FXDECONV and DnCNN. This advantage was demonstrated through both qualitative and quantitative evaluations of the structure of the reconstructed images.

Application of the modified U-Net architecture to real-world data with different noise characteristics

The results of applying the modified U-Net architecture to real-world data showed that the previously established reconstruction properties were preserved not only under controlled synthetic testing conditions but also when processing images with different noise intensity, structure, and frequency content (Ronneberger *et al.*, 2015). Analysis of three datasets revealed that the algorithm's performance was not limited to a single reconstruction type. Depending on the characteristics of the input image, differences were evident in three practical testing modes: with pronounced noise contamination, with a relatively clean signal, where reconstruction required more careful noise suppression, and with a mixed-mode distortion, combining random and locally coherent noise. In this regard, the Kerry, Volve, and F3 datasets were considered not as isolated application examples, but as complementary scenarios for testing the model on heterogeneous input data (Szydlik *et al.*, 2006; Alotaby, 2015; Silva *et al.*, 2019). The first of these scenarios was related to the Kerry dataset, for which the original images were characterised by pronounced noise contamination, which hindered the perception of the useful signal. In this case, the analysis focused on whether the reduction of the random noise component was accompanied by the restoration of the structural readability of the image under conditions of partial masking of useful elements by interference. The obtained results showed that when processing the Kerry data, reconstruction was accompanied not only by a reduction in the visually perceived noise level but also by a clearer representation of the internal organisation of the image. Consequently, individual structural elements were more clearly traced, and the spatial relationships between these elements were recorded more consistently. The result of applying the model to the Kerry data is presented in Figure 2, which compares the original image, the reconstructed result, and the estimated noise component.

As can be seen in Figure 2, the original image was characterised by a high level of noise contamination, as a result of which part of the useful signal was partially masked, and the spatial structure of the image was perceived less clearly. After applying the model, the background noise component was reduced, extended structural lines were more clearly visible, and local variations were reproduced with less interference. The reconstructed image showed no signs of excessive smoothing. Its internal heterogeneity was preserved, while becoming more consistent with the underlying signal rather than to random noise fluctuations. Analysis of the panel with estimated noise revealed that the extracted component contained predominantly chaotic high-frequency and weakly structured elements, while the main extended features of the useful image were largely absent. These results indicated a separation of signal and noise without noticeable disruption of the spatially organised components. In other words, the model reduced not the overall image variability as such, but primarily that portion of it related to noise contamination, while preserving the fundamental signal geometry in the reconstructed result. In other words, for the intense noise scenario, this was reflected in a reduction in the noise level while maintaining the structural coherence of the image. The result obtained on the Kerry dataset characterised the first mode of model validation on real data, namely processing an image with pronounced noise masking. In this case, the reconstruction effect was primarily evident in the restoration of seismic reflective events clarity and the reconstruction of spatial structure. Thus, the Kerry dataset illustrates the model's behaviour in conditions where processing involves mitigating substantial noise contamination while preserving the signal's internal geometry rather than performing minor residual corrections.

The next testing mode was performed using the Volve dataset, for which the original data had a lower level of noise contamination. In this situation, the analysis shifted from the severity of noise reduction to the degree of preservation of weak and already distinguishable structural details after reconstruction. The corresponding visual result was presented in Figure 3.

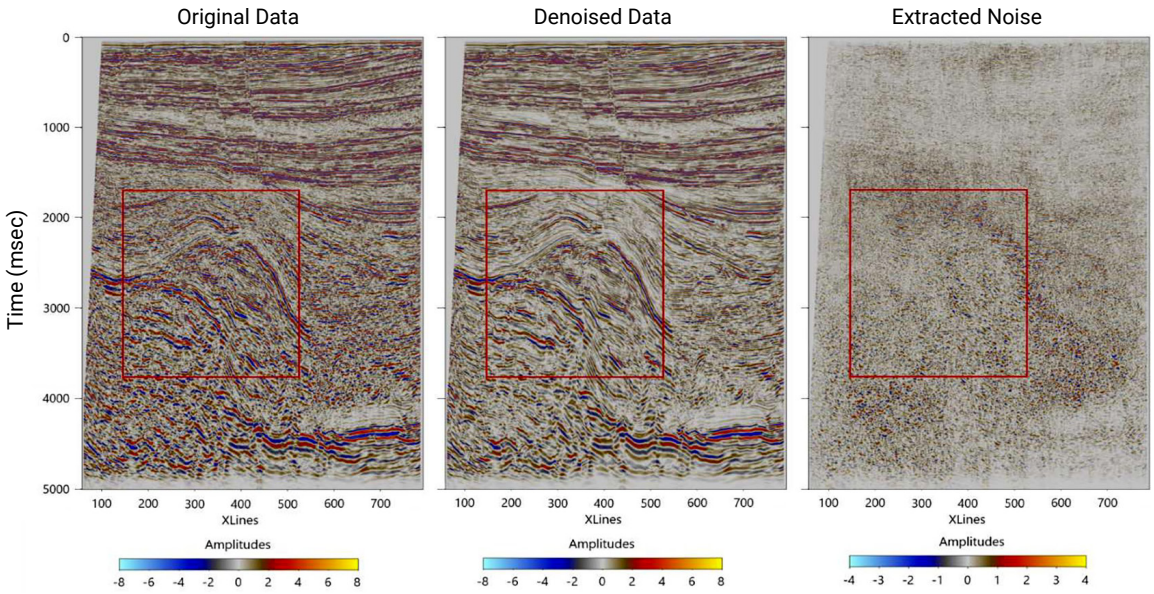

Figure 2. The result of applying the model to real Kerry data: original image, reconstructed image, and estimated noise
Note: the colour range used to estimate the noise level is compressed by half. Red rectangles highlight fragments for visual comparison of changes in the signal structure after processing. The colour scale reflects the amplitude distribution in the original image, reconstructed data, and the extracted noise component
Source: based on T.J. Szydlik *et al.* (2006), W.D.M. Alotaby (2015), R.M. Silva *et al.* (2019)

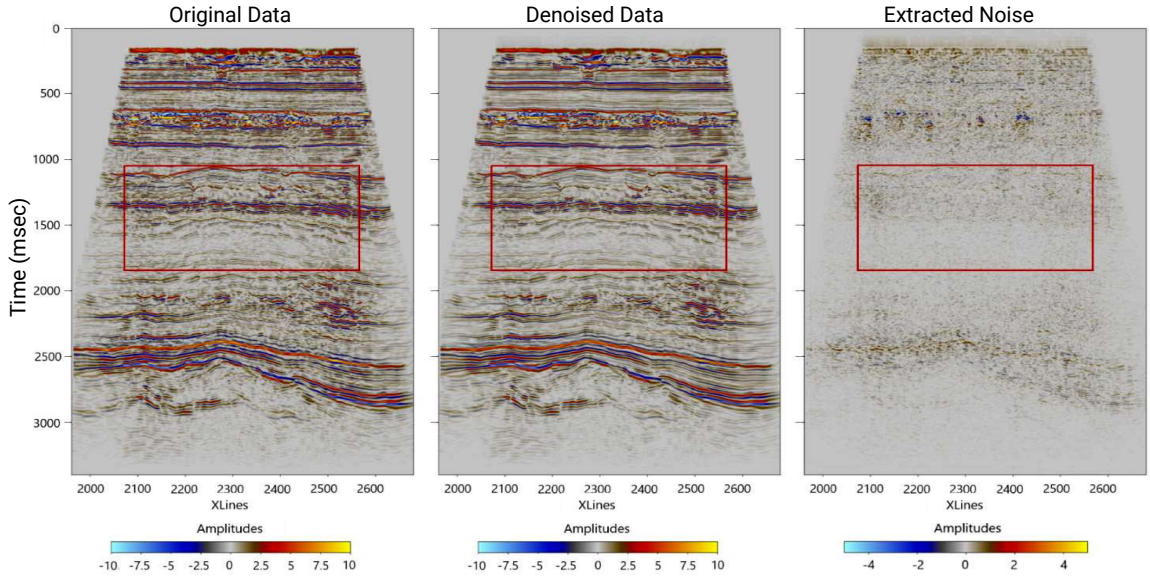

Figure 3. The result of applying the model to real Volve data: original image, reconstructed image, and estimated noise
Source: based on T.J. Szydlik *et al.* (2006), W.D.M. Alotaby (2015), R.M. Silva *et al.* (2019)

As can be seen in Figure 3, in the case of the Volve dataset, the original image was characterised by a lesser degree of noise masking of reflective events compared to the intense noise contamination scenario. In this setting, the reconstruction result was assessed not so much by the degree of noise suppression as by the preservation of already distinguishable structural details. After applying the model, the main seismic events retained the continuity and geometry, while the small-scale chaotic component within the selected area was reduced. At the same time, local transitions, low-contrast elements, and the configuration of seismic reflection events remained distinguishable. The estimated noise component contained predominantly scattered, weakly structured fluctuations and did not reproduce the extended elements of the primary signal. This indicated that the processing in this case was focused on reducing residual noise without disrupting the internal structure of the image. Overall, the results on the Volve dataset characterised a different operating mode of the model compared to the Kerry case: whereas

in the former case, the main effect was associated with reducing pronounced noise masking, here, reconstruction manifested itself in local correction of the residual noise component while preserving the already discernible signal structure without introducing artefacts. The third testing mode was represented by the F3 dataset, which was characterised by a non-uniform complex spatial organisation of noise distortions. In this case, reconstruction included both reducing the random noise component and separating the useful true signal from more structured distortions while preserving the geometry of the reflective events. The corresponding result was shown in Figure 4.

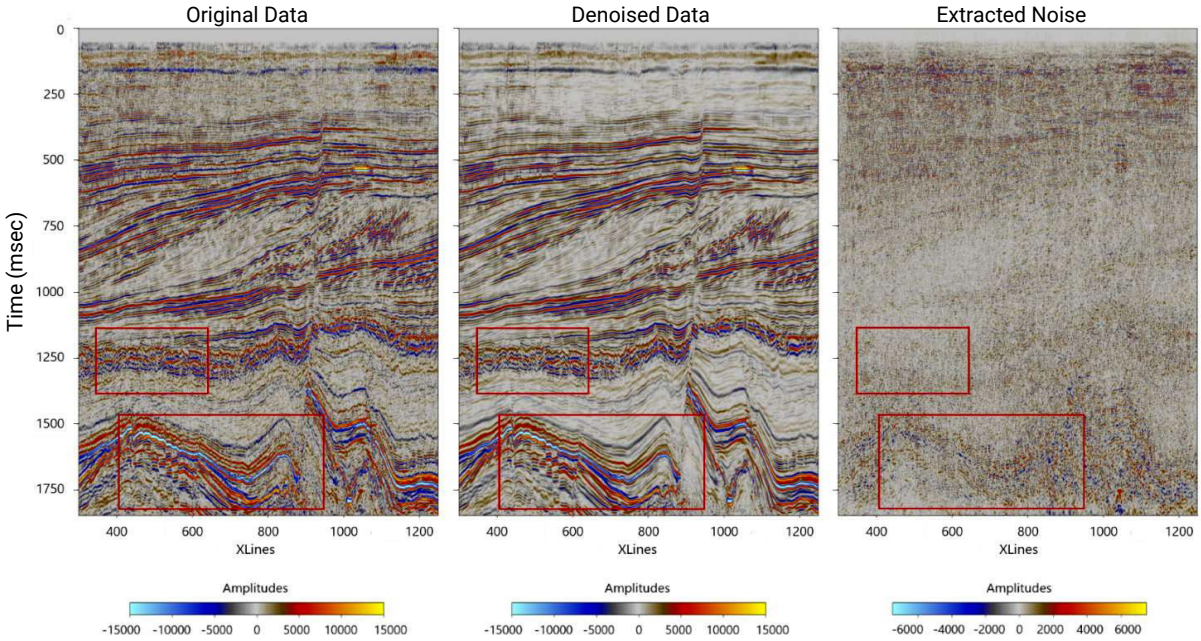

Figure 4. The result of applying the model to real F3 data: original image, reconstructed image and estimated noise
Source: based on T.J. Szydlik *et al.* (2006), W.D.M. Alotaby (2015), R.M. Silva *et al.* (2019)

As can be seen in Figure 4, the F3 dataset was characterised by a non-uniform noise distortion configuration compared to previous cases, as it combined random and more organised noise components. In this formulation, the reconstruction task was associated not only with reducing the overall level of noise variability, but also with separating structurally non-uniform distortions from the main seismic signal. After applying the model, the overall level of the noise component decreased, while the main reflection elements retained visual continuity and spatially consistent. This indicated that the reconstruction addressed not only the chaotic background, but also the more organised noise components without noticeably disrupting the internal structure of the signal. Analysis of the panel with estimated noise showed that both random and locally coherent interfering elements were converted into the noise component, while spatially significant contours, boundaries, and local texture variations were preserved in the reconstructed image. This indicated the model's performance under mixed-distortion conditions, where the boundary between the useful and unwanted components is less obvious. Thus, the result on F3 complemented the two previous testing scenarios: while the main effect on Kerry was restoring readability under significant noise masking, and on Volve, reducing residual noise while preserving the already discernible structure, on F3, reconstruction was associated with separating the useful signal from inhomogeneous noise components under conditions of the mixed spatial organisation. Comparison of the results for Kerry, Volve, and F3 showed that the reconstruction pattern was preserved under three different noise degradation regimes of real data. In the first case, reconstruction involved reducing intense noise masking, in the second, correction with a relatively clean signal, and in the third, processing mixed random and coherent distortions. Thus, the results demonstrated that the reconstruction features were reproduced with varying degrees and spatial organisation of noise.

Spectral analysis of image denoising results

Spectral analysis results showed that after applying the modified U-Net architecture to all three datasets, the amplitude of noise-related components was reduced while maintaining the general shape of the spectral distribution in the informative frequency range. This indicated a reduction in noise energy without significantly altering the spectral components associated with the useful signal. In this case, spectral characteristics were used as an additional tool to verify whether denoising preserved signal structure not only at the visual but also at the frequency level. The averaged amplitude spectra of the original and reconstructed data for the Kerry, Volve, and F3 datasets were presented in Figure 5.

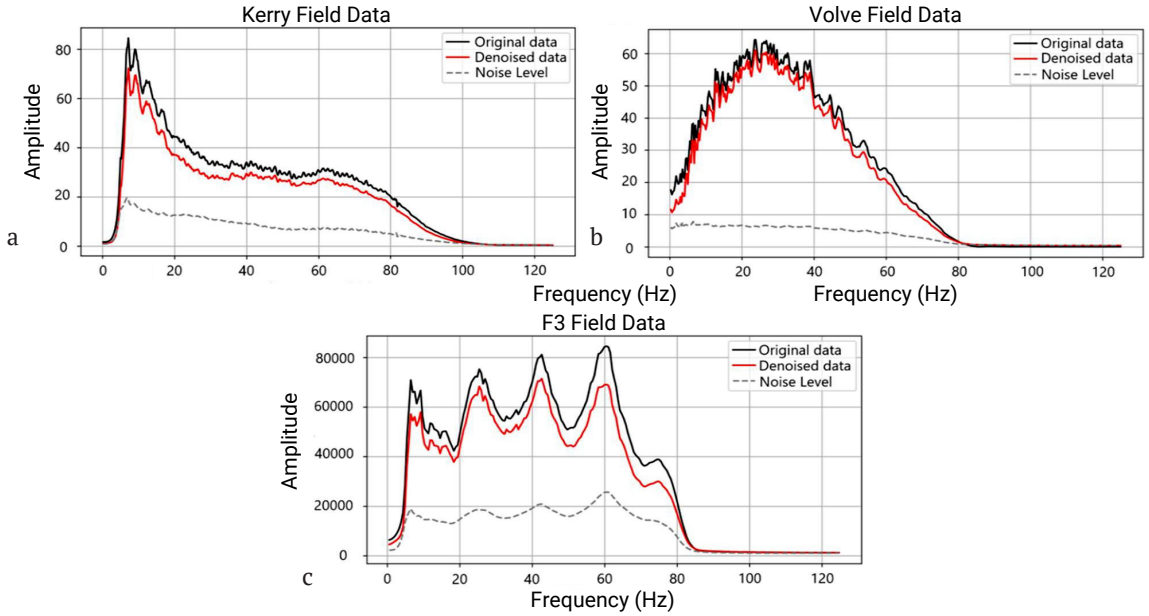

Figure 5. Averaged Fourier amplitude spectra over the entire time interval for the Kerry (a), Volve (b) and F3 (c) sets: original data, noise reduction result and estimated noise component
Source: based on T.J. Szydlik *et al.* (2006), W.D.M. Alotaby (2015), R.M. Silva *et al.* (2019)

As shown in Figure 5, for all three datasets, a reduction in spectral amplitude in the region associated with the noise component was observed after noise reduction, while the spectral configuration in the informative frequency range was preserved. A graphical comparison of the original data, the reconstructed result, and the estimated noise component revealed that the main differences between the curves were concentrated in the part of the spectrum where the noise contribution remained most pronounced, while these differences diminished as the curves approached the upper limit of the working range. For Kerry, discrepancies between the original and reconstructed data were observed up to approximately 100 Hz, where a decrease in amplitude was observed after processing. However, the basic shape of the spectrum in the working range was preserved, and the position of characteristic sections of the curve did not change significantly. For Volve, the changes were less pronounced and the discrepancy between the curves was noted primarily up to 80 Hz, after which the curves converged. These results indicated a reduction in the residual noise component without a noticeable change in the informative portion of the spectrum, and corresponded to a data processing mode with less pronounced noise contamination. For F3, a similar pattern persisted under conditions of non-uniform interference organisation, where a reduction in amplitude after processing was observed across almost the entire operating range up to approximately 85 Hz. Moreover, the dotted curve representing the estimated noise component exhibits a lower amplitude compared to the spectra of the original and reconstructed data, further reflecting the redistribution of energy after processing. This indicated that the reconstruction process attenuates both random and partially structured noise components without changing the overall shape of the spectrum in the region associated with the useful signal. Thus, the spectral data for Kerry, Volve, and F3 showed that reconstruction effectively reduced the noise component while preserving the main characteristics of the useful signal. Taken together, the quantitative, qualitative, and spectral results demonstrated that the modified U-Net architecture and the computational framework implemented on its basis ensured the reconstruction of noisy images across a range of noise intensities and distortion types. On synthetic data, this was reflected in improved SNR, PSNR, and MS-SSIM values relative to FXDECONV and DnCNN, while on real data it was evidenced by the consistent reproduction of reconstruction patterns under varying noise degradation conditions. The obtained results indicated that the proposed approach under consideration was aimed not only at reducing the noise component but also at preserving the spatial organisation of the image, local boundaries, transitions, and spectrally significant signal characteristics. Seismic data were used as a representative application example to evaluate the method on images with complex internal structures and heterogeneous noise patterns. Overall, this formulation allowed considering the proposed computational framework as a generalisable approach, applicable beyond seismic data to a broader range of problems that required both reduction of the noise component and preservation of the structural integrity in reconstructed images.

Discussion

The obtained results showed that the performance of the modified U-Net architecture was characterised not only by effective suppression of the noise component, but also by preservation of spatially organised image structures. These findings were consistent with the results of T. Zhong *et al.* (2022), where a deep residual U-Net architecture was

also accompanied by random noise attenuation while preserving reflective events and geometric consistency. This comparison indicated a relationship between the use of the U-Net architecture with residual connections and the simultaneous attenuation of noise energy and the preservation of the internal structure of the signal. The combination of multi-level feature extraction with skip and residual connections facilitated the separation of the noise component from the useful content without pronounced smoothing. Quantitative evaluation on synthetic data showed higher values of the SNR, PSNR, and MS-SSIM compared to the baseline methods. These observations aligned with the more general results of Z. Wu *et al.* (2025), where improvements in the quality of reconstruction were also considered as a consequence of the simultaneous correction of noise distortions and the preservation of the structural characteristics of the image in the frequency domain. In this study, these differences were particularly evident for data, in which the spatial organisation of the signal was important for interpretation. Unlike general image restoration tasks, where emphasis was often placed on overall reconstruction fidelity, structurally complex images require the preservation of low-contrast yet spatially consistent features. Accordingly, the advantages of the proposed method were reflected not only in quantitative metrics, but also in visual reconstruction quality, where noise reduction does not compromise local transitions, contours, or fine details. Analysis of the data presented by Y.-T. Wu & R.R. Stewart (2023) showed similar conclusions, who associated the use of U-Net with attenuation of coherent noise, while preserving the structural integrity of seismic data. In both cases, neural network reconstruction was accompanied by a reduction in noise while preserving the informative signal. This suggested that the U-Net architecture can be considered as a tool for separating spatially organised useful and parasitic components. Analysis of real data further demonstrated that the nature of the reconstruction was preserved under several noise degradation conditions, such as pronounced noise contamination, low noise presence, and with a mixed nature of distortions. This robustness was consistent with the findings of F.K. Anjom *et al.* (2024), according to which modern machine learning methods in seismic exploration were characterised by stability with respect to variability in geological and noise conditions. Overall, the results suggest that the proposed neural network framework provides not only high accuracy under controlled conditions but also reliable and reproducible performance on heterogeneous real-world data. Controlled variability of training pairs and noise contamination ranges ensured the formation of a more generalised scheme for separating signal and interference.

The obtained results showed that, when processing the Kerry dataset, the main reconstruction effect was manifested in the restoration of the readability of reflective events under conditions of intense noise masking, whereas for Volve, a more local correction of residual noise predominated, and for F3, a stable separation of random and more organised distortions. These findings partially correlated with the results of H. Tang *et al.* (2023), where the RRU-net (residual recurrent U-Net) architecture was used for simultaneous reconstruction and noise reduction of complex data obtained by the distributed acoustic sensing method in vertical seismic profiling. In both cases, the neural network approach demonstrated effectiveness not only within a single distortion regime, but under conditions of a more complex and structurally complex input data. The key difference was determined by the specificity of the source material: in the case of distributed acoustic sensing data, the spatial organisation of the signal and noise had distinct characteristics, whereas this study, the stability of the model was assessed on several types of real seismic images with varying levels presence of random and locally-coherent noise. The obtained results showed the effective reduction of the noise component was accompanied by the preservation of the structural integrity of the image and was not reduced to a simple high-frequency smoothing. These findings were consistent with the results of L. Yang *et al.* (2021), where an improved residual convolutional neural network provided random noise suppression, while preserving main events. The agreement across studies suggested that architectures with residual mechanisms provided a balance between noise suppression and preservation of signal. This can be explained by the role of residual connections, which increased the stability of feature extraction and reduced the risk of losing weak, but meaningfully significant image elements. Comparison with the results of H. Xi *et al.* (2026) further confirmed that the effectiveness of U-Net-based architectures in seismic denoising was maintained in more recent modifications aimed for more accurate signal protection in complex noise environments. This research results demonstrated a similar trend, as reconstruction was accompanied by a reduction in the noise level without significant degradation of the primary signal content. However, the emphasis here extended beyond noise suppression alone, and also on the stability and generalisation of the effect under various degradation conditions in real data. This distinction reflected a broader analytical framework, integrating synthetic, visual, and spectral evaluations rather than focusing solely on the performance of a specific environment.

The results showed that the reconstruction process was learned under supervised training conditions using "noisy image/clean image" pairs, in which the model was trained to establish a direct mapping between degraded and original signals. This formulation was consistent with the adopted methodological framework and supported the interpretation of improvements in SNR, PSNR, and MS-SSIM as outcomes of supervised learning. This approach differed from that of J. Lehtinen *et al.* (2018), where Noise2Noise was an unsupervised approach to restore images without clean reference data. The distinction lain in the nature of the training information: in supervised settings, reconstruction relied on explicit correspondence between noisy and clean signals, whereas Noise2Noise exploited the

statistical consistency across multiple noisy realisations of the same image. A similar contrast can be drawn with the work of J. Batson & L. Royer (2019), where self-supervised denoising strategies were employed without an explicit ground-truth reference. In this study, the use of supervised training pairs was accompanied by a change in quantitative indicators on synthetic data and preservation of the nature of reconstruction when applied to real images. For structurally complex data with a heterogeneous noise background, the presence of a reference target provided a straightforward scheme for separating useful and parasitic components while preserving spatially significant elements.

Differences among noise reduction approaches were evident not only in comparison with classical methods but also relative to early convolutional models. In the work of X. Si *et al.* (2019), convolutional neural networks were applied to attenuate random noise in seismic data, reflecting a similar objective of separating useful signal from noise. However, in this study, reconstruction was addressed more broadly, such as not merely as denoising, but as the preservation of both spatial and spectral organisation. This perspective was consistent with the model design, where skip and residual connections support the retention of internal image structure during reconstruction. An alternative formulation was presented by A. Krull *et al*. (2019), where noise reduction was achieved without clean reference data through self-supervised learning on single noisy images. In contrast, the approach considered here relied on supervised training with explicit correspondence between degraded and reference data, enabling more direct separation of useful and spurious elements. A related emphasis appeared in the work of T. Garber & T. Tirer (2024), where image restoration was evaluated not only by error reduction but also by preservation of meaningful signal content. In this study, the distinction lain primarily in the computational implementation, as the modified U-Net with skip and residual connections provided a specific mechanism for achieving this balance. Similar principles extended to more recent architectures. In the work of S.W. Zamir *et al.* (2022), the Restormer model was designed to restore high-resolution images by capturing long-range dependencies. As in the present case, reconstruction goes beyond local smoothing across multiple representation levels. However, while transformer-based models emphasised global context modelling, the approach here relied on multi-level convolutional feature extraction combined with skip connections and residual refinement. Another direction was illustrated by V. Potlapalli *et al.* (2023) with PromptIR, which targeted multiple degradation types within a single framework. A partial similarity can be observed in the stability of reconstruction across different noise conditions in this study, from strong contamination to mixed distortions. Nevertheless, PromptIR was inherently designed as a general-purpose restoration model that operated without predefined degradation types and incorporated a prompting mechanism. In contrast, the present framework addressed a more specific denoising task, with emphasis on preserving signal structure under defined noise conditions. Overall, the key distinction lain in the scope of applicability: generalised model aimed to handle diverse degradation types within a unified architecture, whereas the proposed approach focused on accurate reconstruction within a specified noise regime while maintaining structural fidelity.

Conclusions

The study presented a method for image quality enhancement though noise removal using the modified U-Net architecture and synthetic images for training purpose. On synthetic blind test images, the proposed methodology achieved a higher quantitative performance compared to FXDECONV and DnCNN. On real data, it consistently maintained the reconstruction quality across a range of noise degradation conditions. This was reflected in the accurate restoration of intensity characteristics, as well as the preservation of edges, variations in local features, morphology, and the relative spatial arrangement of structural elements, without introducing smoothing effect. A quantitative comparison on synthetic test images revealed clear differences between the methods across the main reconstruction metrics. The proposed approach achieved average values of 45.9 dB for SNR, 29.7 dB for the PSNR, and 0.99 for the MS-SSIM. In comparison, FXDECONV yielded 31.5 dB, 23.9 dB, and 0.94, while DnCNN produced 20.9 dB, 18.4 dB, and 0.86, respectively. These differences indicated improvements not only in noise suppression, but also in intensity fidelity and preservation of spatial structure of the image. When applied to real data, the method demonstrated consistent reconstruction behaviour across multiple noise degradation scenarios. For the Kerry dataset, this was reflected in reduced noise masking and improved visibility of structural features. For Volve, it was expressed as a decrease in residual noise while preserving the already distinguishable signal structure. In the case of F3, stable performance was maintained despite more complex spatial interference patterns. Spectral analysis further confirmed that reconstruction, across all three datasets was associated with attenuation of the noise content without altering the overall spectral structure within the main frequency bandwidth. Taken together, obtained results demonstrated that the modified U-Net architecture was applicable for denoising and reconstructing structurally complex images. The combination of encoding and decoding components, skip, and residual corrections enabled noise reduction without significantly disrupting the image. These findings supported the applicability of the proposed approach beyond seismic data to other types of noisy images, for which simultaneous noise suppression and preservation of fine scale detail was crucial. The study was limited by the finite number of datasets analysed, and the model was tested primarily under noise-based distortion conditions, without addressing a wider range of combined image degradations. Further research may include expanding the dataset diversity, evaluating robustness under more complex distortion scenarios, and comparing

performance with other modern reconstruction architectures across varied image degradation conditions.

Acknowledgements
None.

Funding
None.

Conflict of Interest
None.

References

[1] Alotaby, W.D.M. (2015). *Fault interpretation and reservoir characterization of the Farewell formation within Kerry Field, Taranaki Basin, New Zealand*. (Master's thesis, Missouri University of Science and Technology, Rolla, USA).
[2] Anjom, F.K., Vaccarino, F., & Socco, L.V. (2024). Machine learning for seismic exploration: Where are we and how far are we from the holy grail? *Geophysics*, 89(1), 157-178. doi: 10.1190/geo2023-0129.1.
[3] Azizova, S., Mammadova, S., Hasanov, J., & Aliyeva, S. (2026). Qualitative analysis of medical image colorization with the realistic color palette adjustment. *Problems of Information Technology*, 17(1), 23-31. doi: 10.25045/jpit.v17.i1.03.
[4] Batson, J., & Royer, L. (2019). Noise2Self: Blind denoising by self-supervision. In *Proceedings of the 36th international conference on machine learning*. California: PMLR 97.
[5] Canales, L.L. (1984). Random noise reduction. In *Proceedings of the SEG technical program expanded abstracts 1984* (pp. 525-527). New York: American Society of Mechanical Engineers. doi: 10.1190/1.1894168.
[6] Cui, Y., Ren, W., Cao, X., & Knoll, A. (2024). Revitalizing convolutional network for image restoration. *IEEE Transactions on Pattern Analysis and Machine Intelligence*, 46(12), 9423-9438. doi: 10.1109/TPAMI.2024.3419007.
[7] Ding, M., Zhou, Y., & Chi, Y. (2024). Seismic signal denoising using Swin-Conv-UNet. *Journal of Applied Geophysics*, 223, article number 105355. doi: 10.1016/j.jappgeo.2024.105355.
[8] Garber, T., & Tirer, T. (2024). Image restoration by denoising diffusion models with iteratively preconditioned guidance. In *IEEE/CVF conference on computer vision and pattern recognition* (pp. 25245-25254). Seattle: IEEE Computer Society. doi: 10.1109/CVPR52733.2024.02385.
[9] Goyal, B., Dogra, A., Agrawal, S., Sohi, B.S., & Sharma, A. (2020). Image denoising review: From classical to state-of-the-art approaches. *Information Fusion*, 55, 220-244. doi: 10.1016/j.inffus.2019.09.003.
[10] Gülünay, N. (1986). FXDECON and complex wiener prediction filter. In *Proceedings of the SEG technical program expanded abstracts 1986* (pp. 279-281). New York: American Society of Mechanical Engineers. doi: 10.1190/1.1893128.
[11] He, K., Zhang, X., Ren, S., & Sun, J. (2016). Deep residual learning for image recognition. In *IEEE conference on computer vision and pattern recognition* (pp. 770-778). Las Vegas: IEEE. doi: 10.1109/CVPR.2016.90.
[12] Imamverdiyev, Y.N., & Musayeva, F.I. (2022). Analysis of generative adversarial networks. *Problems of Information Technology*, 13(1), 20-27. doi: 10.25045/jpit.v13.i1.03.
[13] Kingma, D.P., & Ba, J.L. (2015). Adam: A method for stochastic optimization. In *3rd international conference on learning representations*. San Diego, USA. doi: 10.48550/arXiv.1412.6980.
[14] Krull, A., Buchholz, T.-O., & Jug, F. (2019). Noise2Void – learning denoising from single noisy images. In *IEEE/CVF conference on computer vision and pattern recognition* (pp. 2129-2137). Piscataway: IEEE.
[15] Lehtinen, J., Munkberg, J., Hasselgren, J., Laine, S., Karras, T., Aittala, M., & Aila, T. (2018). Noise2Noise: Learning image restoration without clean data. In *Proceedings of the 35th international conference on machine learning*. Stockholm: PMLR.
[16] Luo, Z., Gustafsson, F.K., Zhao, Z., Sjölund, J., & Schön, T.B. (2025). Taming diffusion models for image restoration: A review. *Philosophical Transactions of the Royal Society A: Mathematical, Physical and Engineering Sciences*, 383(2299), article number 20240358. doi: 10.1098/rsta.2024.0358.
[17] Mao, J., Sun, L., Chen, J., & Yu, S. (2025). Overview of research on digital image denoising methods. *Sensors*, 25(8), article number 2615. doi: 10.3390/s25082615.
[18] Nazir, N., Sarwar, A., & Saini, B.S. (2024). Recent developments in denoising medical images using deep learning: An overview of models, techniques, and challenges. *Micron*, 180, article number 103615. doi: 10.1016/j.micron.2024.103615.
[19] Potlapalli, V., Zamir, S.W., Khan, S., & Khan, F.S. (2023). PromptIR: Prompting for all-in-one blind image restoration. In *Proceedings of the 37th international conference on neural information processing systems* (pp. 71275-71293). Red Hook: Curran Associates, Inc. doi: 10.5555/3666122.3669243.
[20] Ronneberger, O., Fischer, P., & Brox, T. (2015). U-Net: Convolutional networks for biomedical image segmentation. In N. Navab, J. Hornegger, W. Wells & A. Frangi (Eds.), *Medical image computing and computer-assisted intervention – MICCAI 2015* (pp. 234-241). Cham: Springer. doi: 10.1007/978-3-319-24574-4_28.
[21] Si, X., Yuan, Y., Si, T., & Gao, S. (2019). Attenuation of random noise using denoising convolutional neural networks. *Interpretation*, 7(3), 269-280. doi: 10.1190/INT-2018-0220.1.
[22] Silva, R.M., Baroni, L., Ferreira, R.S., Civitarese, D., Szwarcman, D., & Brazil, E.V. (2019). Netherlands dataset: A new public dataset for machine learning in seismic interpretation. *arXiv*. doi: 10.48550/arXiv.1904.00770.

[23] Szydlik, T.J., Way, S., Smith, P., Aamodt, L., & Friedrich, C. (2006). 3D PP/PS prestack depth migration on the Volve field. In *68th EAGE conference and exhibition incorporating SPE EUROPEC 2006* (cp-2-00185). Houten: European Association of Geoscientists & Engineers. doi: 10.3997/2214-4609.201402177.

[24] Tang, H., Cheng, S., Li, W., & Mao, W. (2023). Simultaneous reconstruction and denoising for DAS-VSP seismic data by RRU-net. *Frontiers in Earth Science*, 10, article number 993465. doi: 10.3389/feart.2022.993465.

[25] Tian, C., Fei, L., Zheng, W., Xu, Y., Zuo, W., & Lin, C.-W. (2020). Deep learning on image denoising: An overview. *Neural Networks*, 131, 251-275. doi: 10.1016/j.neunet.2020.07.025.

[26] Wang, Z., Simoncelli, E.P., & Bovik, A.C. (2003). Multiscale structural similarity for image quality assessment. In *The thrity-seventh asilomar conference on signals, systems & computers* (pp. 1398-1402). Pacific Grove: IEEE. doi: 10.1109/ACSSC.2003.1292216.

[27] Wu, Y.-T., & Stewart, R.R. (2023). Attenuating coherent environmental noise in seismic data via the U-net method. *Frontiers in Earth Science*, 11, article number 1082435. doi: 10.3389/feart.2023.1082435.

[28] Wu, Z., Liu, W., Wang, J., Li, J., & Huang, D. (2025). FrePrompter: Frequency self-prompt for all-in-one image restoration. *Pattern Recognition*, 161, article number 111223. doi: 10.1016/j.patcog.2024.111223.

[29] Xi, H., Luo, J., Liu, J., Shi, W., Chen, G., Wang, N., & Huang, X. (2026). MSBE-UNet: A deep learning denoising method for effective seismic noise suppression. *Acta Geophysica*, 74, article number 65. doi: 10.1007/s11600-026-01799-3.

[30] Xia, B., Zhang, Y., Wang, S., Wang, Y., Wu, X., Tian, Y., Yang, W., & Van Gool, L. (2023). DiffIR: Efficient diffusion model for image restoration. In *IEEE/CVF international conference on computer vision* (pp. 13049-13059). Paris: IEEE. doi: 10.1109/ICCV51070.2023.01204.

[31] Yang, L., Chen, W., Wang, H., & Chen, Y. (2021). Deep learning seismic random noise attenuation via improved residual convolutional neural network. *IEEE Transactions on Geoscience and Remote Sensing*, 59(9), 7968-7981. doi: 10.1109/TGRS.2021.3053399.

[32] Zamir, S.W., Arora, A., Khan, S., Hayat, M., Khan, F.S., & Yang, M.-H. (2022). Restormer: Efficient transformer for high-resolution image restoration. In *IEEE/CVF conference on computer vision and pattern recognition* (pp. 5728-5739). New Orleans: IEEE. doi: 10.1109/CVPR52688.2022.00564.

[33] Zhang, K., Zuo, W., Chen, Y., Meng, D., & Zhang, L. (2017). Beyond a gaussian denoiser: Residual learning of deep CNN for image denoising. *IEEE Transactions on Image Processing*, 26(7), 3142-3155. doi: 10.1109/TIP.2017.2662206.

[34] Zhao, H., Gallo, O., Frosio, I., & Kautz, J. (2017). Loss functions for image restoration with neural networks. *IEEE Transactions on Computational Imaging*, 3(1), 47-57. doi: 10.1109/TCI.2016.2644865.

[35] Zhong, T., Cheng, M., Dong, X., Li, Y., & Wu, N. (2022). Seismic random noise suppression by using deep residual U-Net. *Journal of Petroleum Science and Engineering*, 209, article number 109901. doi: 10.1016/j.petrol.2021.109901.

Застосування методів глибокого навчання для обробки та покращення зображень: тематичне дослідження сейсмічних даних

Руслан Маліков

Аспірант
Інститут геології та геофізики Національної академії наук Азербайджану
AZ1143, просп. Х. Джавіда, 119, м. Баку, Азербайджан
https://orcid.org/0009-0005-2126-1642

Анотація. Метою цього дослідження була оцінка ефективності модифікованої архітектури нейронної мережі кодер-декодер для шумозаглушення та покращення зображень з використанням синтетичних та реальних даних. Методологія дослідження базувалася на обчислювальному експерименті та включала навчання моделі на синтетичних зображеннях, кількісне порівняння отриманих результатів за допомогою методу f-x деконволюції та альтернативної моделі згорткового шумозаглушення, а також перевірку стійкості на реальних даних з наявністю різних шумових характеристик. Було виявлено, що застосований метод шумозаглушення характеризувався не тільки зменшенням шумової складової, але й збереженням просторово значущих характеристик зображення, включаючи різкість країв, локальні переходи, морфологію та відносне положення структурних елементів без ознак надмірного розмиття. Остаточне порівняння методів на синтетичних тестових зображеннях показало, що середнє співвідношення сигнал/шум, пікове співвідношення сигнал/шум та багатомасштабний індекс структурної подібності для запропонованого підходу становили 45,9 дБ, 29,7 дБ та 0,99 відповідно. Для методу f-x деконволюції відповідні значення становили 31,5 дБ, 23,9 дБ та 0,94, тоді як для альтернативної моделі згорткового шумозаглушення значення становили 20,9 дБ, 18,4 дБ та 0,86. При застосуванні до реальних даних зберігалася та сама поведінка покращення, включаючи видалення вираженого шумового забруднення та отримання відносно чистого сигналу без спотворень. Залежно від вхідних характеристик, метод супроводжувався зменшенням інтенсивного маскування шуму, зменшенням залишкового шуму зі збереженням чіткої структури сигналу та реконструкцією в умовах більш складної просторової організації перешкод. Спектральний аналіз виявив зменшення енергії шуму без порушення спектральної конфігурації в інформативному діапазоні частот. Практичне значення полягає в потенційному застосуванні запропонованого підходу як обчислювального методу обробки шумних зображень у системах, призначених для шумозаглушення та відновлення різних структур даних

Ключові слова: відновлення зображень; шумозаглушення зображень; структурне збереження; реконструкція сейсмічних зображень; навчання з учителем